Available online at www.sciencedirect.com

SciVerse ScienceDirect

PHOTONICS AND NANOSTRUCTURES Fundamentals and Applications

Photonics and Nanostructures – Fundamentals and Applications 10 (2012) 319–324

www.elsevier.com/locate/photonics

Silicon nitride PhC nanocavities as versatile platform for visible spectral range devices

F. Pisanello [a,b,1,*], L. Martiradonna [c,1], A. Qualtieri [c,1], T. Stomeo [c,1], M. Grande [d], P.P. Pompa [c], R. Cingolani [a,c], A. Bramati [b], M. De Vittorio [a,c]

[a] National Nanotechnology Laboratory, CNR-Istituto di Nanoscienze, Scuola superiore ISUFI, Università del Salento, 16 Via Arnesano, Lecce 73100, Italy

[b] Laboratoire Kastler Brossel, CNRS UMR8552, Université Pierre et Marie Curie, Ecole Normale Supérieure, 4 Place Jussieu, 75252 Paris Cedex 05, France

[c] Center for Bio-Molecular Nanotechnology, Istituto Italiano di Tecnologia (IIT), Via Barsanti 1, Arnesano, Lecce 73010, Italy

[d] Dipartimento di Elettrotecnica ed Elettronica, Politecnico di Bari, Via Re David 200, 70125 Bari, Italy

Received 30 December 2010; received in revised form 4 June 2011; accepted 12 August 2011

Available online 22 August 2011

Abstract

We propose silicon nitride two-dimensional photonic crystal resonators as flexible platform to realize photonic devices based on spontaneous emission engineering of nanoemitters in the visible spectral range. The versatility of our approach is demonstrated by coupling the two dipole-like modes of a closed band gap H1 nanocavity with: (i) DNA strands marked with Cyanine 3 organic dyes, (ii) antibodies bounded to fluorescent proteins and (iii) colloidal semiconductor nanocrystals localized in the maximum of the resonant electric field. The experimental results are in good agreement with the numerical simulations, highlighting the good coupling of the nanocavities with both organic and inorganic light emitters.

Keywords: Photonic crystals nanocavity; Visible; DNA; Nanocrystals

1. Introduction

Two-dimensional (2D) photonic crystal (PhC) technology is well established at telecommunication bands, and materials such as silicon (Si), gallium arsenide (GaAs) or indium phosphide (InP) represent a common solution for applications at these wavelengths [1–4]. However the interest of scientific community on structures operating in other spectral regions, such as the visible one, is growing up for both linear and non-linear applications [5–7]. Indeed, 2D-PhC cavities resonating in the visible spectral range are considered a promising tool to boost photonic device performances in several fields, such as biosensing, integrated optics, quantum communications, solar energy, etc. As consequence of this wide area of interest, a photonic platform able to answer to the needs of all these fields would be attractive for scientific and technical communities.

Trying to develop such technological platform, the first problem one should face is the material choice. In principle it should be transparent in the whole visible spectral range with a refractive index (n) relatively high,

* Corresponding author at: Laboratoire Kastler Brossel, CNRS UMR8552, Université Pierre et Marie Curie, Ecole Normale Supérieure, 4 Place Jussieu, 75252 Paris Cedex 05, France.
Tel.: +33 1 44 27 72 66l; fax: +33 1 44 27 38 45.
E-mail address: ferruccio.pisanello@unisalento.it (F. Pisanello).

[1] These authors contributed equally to the work.

1569-4410/$ – see front matter © 2011 Elsevier B.V. All rights reserved.
doi:10.1016/j.photonics.2011.08.003

low cost, compatible with silicon (Si) based technologies, robust, biocompatible and simply functionalizable with several biological species.

In past years several materials have been proposed with this purpose; among them, of remarkable interest are gallium nitride (GaN) [8], gallium phosphide (GaP) [9], polymers [10] and silicon dioxide (SiO_2) [11]. Another appealing material is silicon nitride (Si_3N_4), which answers to most of the above-mentioned requirements. Indeed, stoichiometric silicon nitride is transparent in the visible spectral range with a refractive index $n \sim 1.93$ (@ $\lambda = 600$ nm) [12–14], it can be grown on Si with low cost and widely diffused growth facilities such as plasma enhanced chemical vapor deposition (PECVD) [15], it is compatible with Si based electronics (it is used as insulator in MOSFET gates [16,17]), it is biocompatible and functionalizable with several proteins [18–20].

Several Si_3N_4 2D-PhC cavities have been already proposed in past years [5,21,22], showing a maximum quality factor (Q) of ~3400 in the case of a double heterostructure nanocavity [22]. Moreover, recent advances in development of nanobeam cavities have led to extremely high quality factors also in the visible [23–25], with a maximum Q of ~55 000 [25]. In this contribution we propose Si_3N_4 PhC resonators as platform to realize photonic devices based on spontaneous emission engineering of nanoemitters in the visible spectral range. The versatility of our approach is demonstrated by coupling the two dipole-like modes of a closed band gap single point defect nanocavity with organic and inorganic light emitters: (i) DNA strands marked with Cyanine 3 (Cy3) organic dyes, (ii) antibodies bounded to fluorescent proteins (TRITC) and (iii) colloidal semiconductor nanocrystals (NCs) localized in the maximum of the resonant electric field. The 2D-PhC nanocavities have been designed by exploiting both frequency and time domain simulations. The fabrication of the devices has been achieved by means of electron beam lithography (EBL) and deep reactive ion etching processes. Scanning electron microscopy (SEM) images were collected on the processed samples in order to check the morphology of the fabricated pattern, while micro-photoluminescence measurements have been carried out to investigate the optical properties of the realized structures.

2. Resonators design

The coupling between a single quantum emitter and a confined optical mode can lead to two different interaction regimes, called strong and weak coupling [26,27]. In particular, in the weak coupling regime the spontaneous emission rate of the uncoupled emitter is modified and, when the emitter is positioned in the maximum of the localized electric field, this modification is quantified by the so called ''Purcell Factor'' [28], i.e. $F_p = 3/(4\pi^2)Q/V(\lambda/n)^3$, where Q and V are the quality factor and the modal volume of the resonant mode, respectively. If $F_p > 1$, the cavity increases the spontaneous emission rate at the resonant wavelength, thus enhancing the emitter luminescence. In order to maximize F_p, it is thus important to have high Q and low V nanocavities.

The resonators reported in this work have been designed according to Ref. [29] by using both frequency and time domain simulation algorithms. Briefly, the photonic band gap was first designed by using a triangular lattice of air holes with period a and radius r in a dielectric material with $n = 1.93$ by means of a plane wave expansion (PWE) algorithm. A single point defect was then implemented by the omission of an air-hole in the lattice (see Fig. 1(a)) and the localized photonic states analyzed by Finite Difference Time Domain method. When realized in Si_3N_4 and without any other modification, this type of nanocavity, called ''H1'', allows two dipole-like states to be localized in the defect [29–32], as shown by the modal profiles reported Fig. 1(b) and (c), called x-pole and y-pole, respectively. As described in Refs. [29,31], the quality factor of these modes can be enhanced by increasing the thickness of the PhC slab up to when the photonic band gap closes, leading to a strong mismatch in the momentum space between the cavity modes and the 2nd guided mode in structure. However, by increasing the slab thickness, the amount of material with higher refractive index expands, thus increasing the modal volume of the confined photonic states. Nevertheless, this does not affect the Purcell factor, that, by virtue of the closed band gap, presents an absolute maximum of $F_p = 78$, obtained for $t = 1.55a$ (see Fig. 1(d)) for both x- and z-pole modes and corresponding to quality factor of ~700 and a modal volume of $\sim 0.68(\lambda/n)^3$. As described with more details in Ref. [29], this value of F_p can be further enhanced for the z-pole mode by slight modifying two neighboring holes around the defect, allowing to reach a theoretical Purcell factor of about 90 with $Q \sim 810$.

3. Coupling with organic emitters

The resonators were realized on a 400 nm thick Si_3N_4 slab deposited on a Si substrate by means of a PECVD technique. The Si_3N_4 layer was then covered

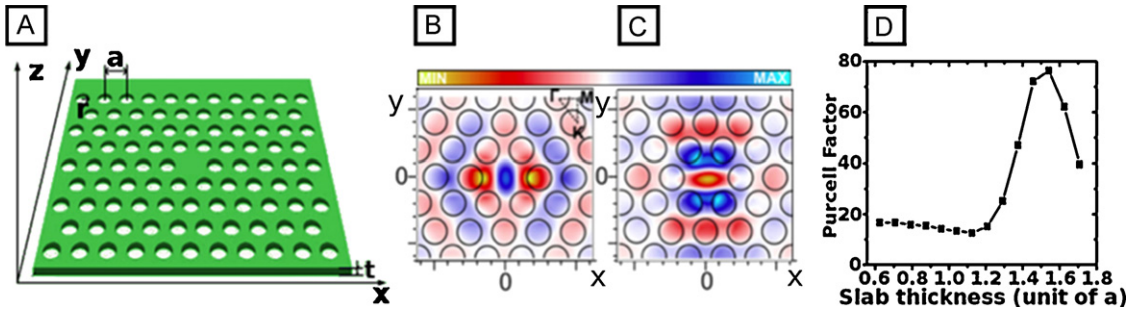

Fig. 1. Closed band gap H1 nanocavity. (a) Sketch of an H1 2D-PhC cavity. (b and c) Spatial dependence of the electric field components E_y and E_x for the x- and y-pole mode, respectively. (d) Dependence of the Purcell factor on the slab thickness.

with 400 nm spin-coated positive e-beam resist and the 2D-PhC pattern defined by EBL with an acceleration voltage of 30 kV and a beam current of 29 pA. The pattern was transferred in the Si_3N_4 dielectric layer by an inductively coupled plasma (ICP) etching process based on a H_2/CF_4 gas mixture. The RF coil power and the RF platen power have been set to 150 W and 50 W, respectively. The membrane structure was then released by wet etching the underlying silicon substrate in a tetramethylammonium hydroxide (TMAH) solution for 10 min at 75 °C. Fig. 2(a) shows scanning electron micrograph (SEM) of the bulk 2D-PhC H1 nanocavity after EBL, ICP and wet etching processes.

Through a solid state bioconjugation chemistry yielding primary amino-groups on the Si_3N_4 surface to link biomolecules, two samples were prepared by covalently immobilizing on PhC resonators (i) single-stranded DNA (ss-DNA) [33] or (ii) antibody probes [34] on the Si_3N_4 surface, respectively. Complementary DNA targets or specific secondary antibodies, labeled with Cyanine 3 (Cy3) and rodhamine (TRITC) fluorophores, respectively, were then allowed to recognize the immobilized probes, thus obtaining a uniform fluorescent monolayer of the biomolecular species. Specifically, the target DNA sequences (match: 5′-Cy3–CTC CCC CAT GCC ATC CTG CG-3′) were left to hybridize with probes for 10 min at 37 °C, while the immune-modified surface was incubated for ∼1 h with a solution of TRITC-coniugated AffiniPure F(ab′)2 Fragment Goat Anti-Mouse IgG (H + L) (concentration 1:200 in 1 × PBS).

In order to characterize the optical properties of the resonators, room temperature micro-photoluminescence (μPL) measurements were carried out. A linear polarizer was introduced in the detection optical path in order to select the y-pole mode, which has the highest quality factor when cavity-neighboring holes are slightly modified as reported in Ref. [29].

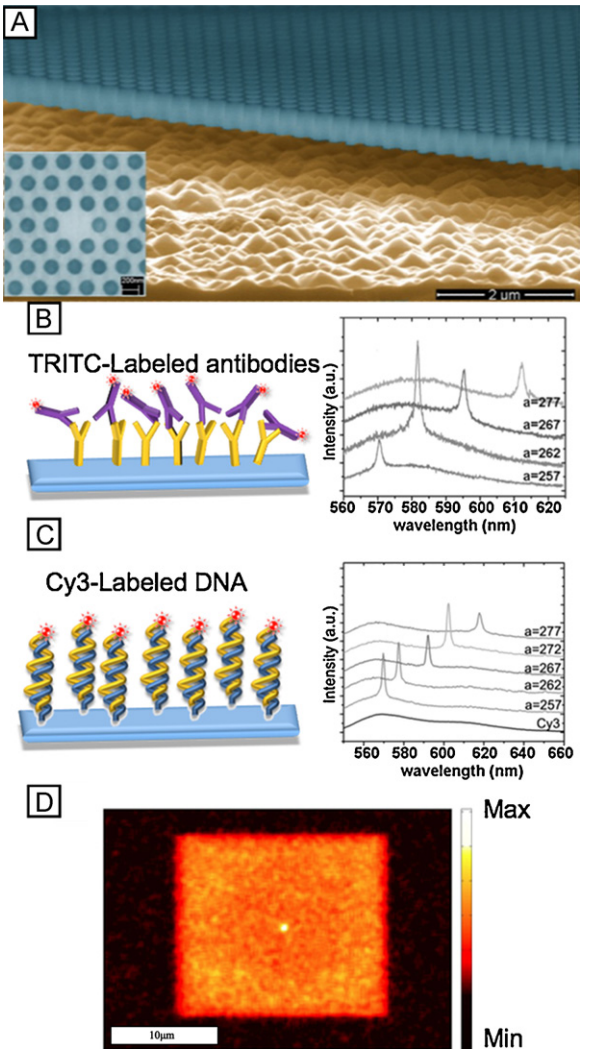

Fig. 2. Organic dyes coupled to PhC cavities. (a) SEM micrograph of the realized resonators. (b and c) Spectral resolved μPL signal collected from Cy3 and TRITC sample, respectively, and for several values of a and $r = 0.308a$. (d) 2D μPL map of a resonant nanocavity.

Fig. 2(b) and (c) display the μPL signal from several nanocavities with different lattice periods: the sharp resonances, superimposed to Cy3 and TRITC luminescence, show a maximum quality factor of $Q \sim 725$ tunable in a wide spectral range. As shown by the bright spot in the center of the 2D spatial μPL map reported in Fig. 2(d), besides improving spectral purity, nanocavities strongly increase dye emission up to 160-fold with respect to the unpatterned substrate. Let us point out that this high emission intensity should be ascribed to the combination of three different phenomena. (i) The presence of the photonic crystal pattern allows probes biomolecules to be functionalized on a wider area, composed by top and bottom surfaces of the resonator and by the walls of the holes. The surface available to probes in the patterned device has been computed to be almost 4 times larger than the one accessible in the flat substrate. (ii) The 2D-PhC pattern introduces extraction channels for the energy confined in the slab, called leaky modes [35,36]. At the same time, the defect region locally modifies light outcoupling by attributing a peculiar radiation pattern to the localized modes [37,38]. (iii) Purcell effect can also modify the emission rate of organic or inorganic emitters interacting with low modal volume, high Q defect modes, further increasing the overall detected emission. In our experiments, we have obtained a 20-fold luminescence increase measured on the square area occupied by the photonic crystal pattern, which is significantly brighter than the unpatterned substrate, as shown by Fig. 2(d). Moreover, a further 8-fold increase as compared to the PhC pattern is obtained in the PhC defect, thus giving a significant overall increase of 160-fold. Exact quantification of the different contributions, and specifically of Purcell effect, would require high spatially-, time- and angle-resolved PL measurements to infer the final emission rate and the radiation patterns of leaky and cavity modes, and is beyond the scope of the present work.

Both spectral tailoring and emission enhancement are key advantages that can boost performances of biodevices based on optical detection of fluorescent marker-labeled bioanalytes. In fact, using these approaches in the optical read-out area of DNA- and protein-chips it is possible to introduce a wavelength multiplexing in the detection process, thus performing ∼150 parallel analysis in a one shot measurement, with a minimum sensitivity increased of a factor as high as 160 [39,40].

4. Coupling inorganic emitters

The same photonic platform has been exploited to efficiently modify the spontaneous emission of colloidal NCs by embedding them in the Si_3N_4 membrane H1 nanocavity. These nanoparticles are considered promising quantum emitter for room temperature single photon generation [41–43], and their coupling with confined optical systems allows to enhance their performances in terms of emission linewidth and radiative lifetime [44]. In order to localize them in the center of the PhC slab, the Si_3N_4 growth procedure has been divided in two stages. In the first one, half of the final Si_3N_4 slab thickness (i.e. $t/2 = 200$ nm) was

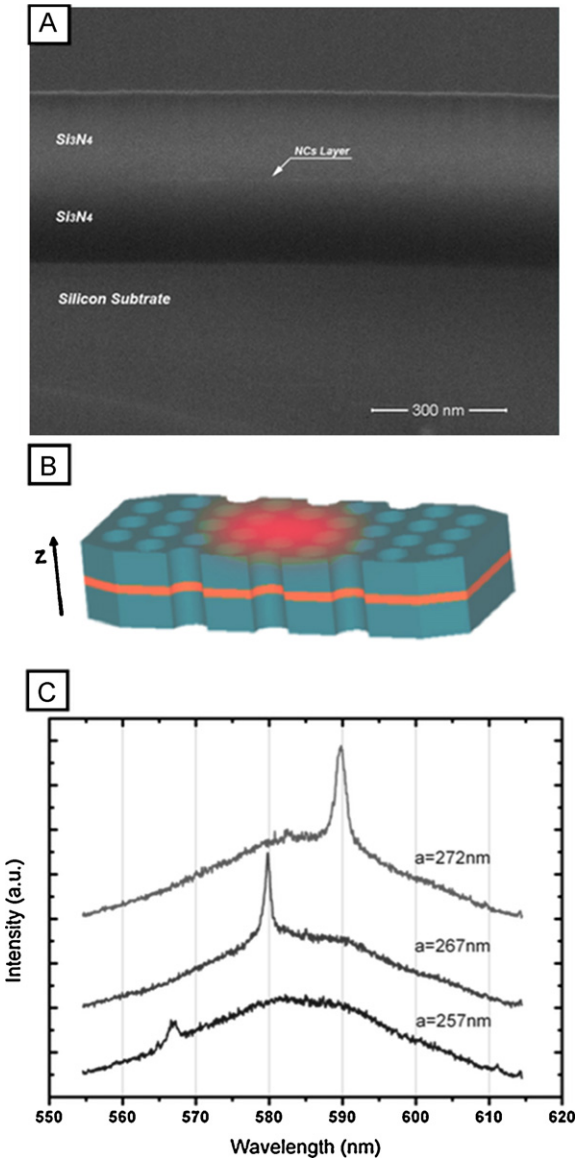

Fig. 3. Colloidal semiconductor nanocrystals embedded in Si_3N_4 PhC resonators. (a) SEM micrograph of the realized sandwiched structure. (b) Sketch of the resonator embedding the colloidal nanocarystal layer. (c) Spectral resolved μPL signal collected from the resonator embedding colloidal NCs for three values of a and $r = 0.308a$.

grown on the Si substrate and a micromolar solution (10^{-6} mol/l) of colloidal CdSe/CdS dot-in-rod nanocrystals [42] in toluene was spin-coated on it [45]. After solvent evaporation, the remaining 200 nm of silicon nitride were grown on the sample. A SEM micrograph of the resulting sandwiched structure is shown in Fig. 3(a). The resonators were then realized through electron bean lithography and dry and wet etching processes as described in Section 3.

By following this approach, in the patterned device (schematized in Fig. 3(b)) the nanoemitters are thus localized in the electric field main lobe, maximizing the Purcell effect and resulting in the resonances reported in Fig. 3(c), which show a maximum quality factor of about 600. The normalized frequency of the experimental results was found to be $a/\lambda \sim 0.46$, against the expected value of a/λ of about 0.431. This slight difference can be mainly imputed to the effects of fabrication imperfections since they induce an added and unavoidable dispersion in the optical properties of the PhCs nanocavities [46]. It is important to underline that the introduction of a guest material sandwiched between two Si_3N_4 layers, does not affect the optical properties of the nanocavity as shown by the good agreement between the calculated and measured Q-factors (equal to 680 and 600, respectively).

5. Conclusions

We have detailed the use of Si_3N_4 2D photonic crystal resonators as flexible platform to realize photonic devices based on spontaneous emission engineering of nanoemitters in the visible spectral range. We have evidenced the versatility of our approach by coupling several types of quantum light emitters to the two photonic states allowed in a closed band gap single point defect nanocavity. In particular, DNA strands and antibodies marked with Cy3 and TRITC organic dyes, respectively, have been immobilized on top of the nanocavities, while colloidal quantum dots emitting in the visible spectral range have been embedded in the resonators and localized in maximum of the localized photonic mode. The optical measurements, carried out by μPL confocal microscopy, revealed maximum quality factors close to the theoretical estimations for all the emitters used in this work.

Improvements in modelling and processing of PhC structures in silicon nitride, which resulted to be highly compatible with both biological materials and inorganic quantum emitters, let us envision a broader application of two-dimensional PhC nanocavities also in the visible spectral range.

Acknowledgements

The authors gratefully acknowledge Iolena Tarantini, Adriana Campa, Giuseppe Vecchio, Gianmichele Epifani and Benedetta Antonazzo for their help in the fabrication process. Financial support from the Italian ministry of instruction, university and research (Project ‘‘FIRB - Hub di ricerca italo-giapponese sulle nanotecnologie’’) is also acknowledged. F.P. and A.B. recognize the support of the French research council ANR under the project SENOQI.

References

[1] T. Tanabe, M. Notomi, S. Mitsugi, A. Shinya, E. Kuramochi, All-optical switches on a silicon chip realized using photonic crystal nanocavities, Appl. Phys. Lett. 87 (2005) 151112.
[2] F. Van Laere, T. Stomeo, C. Cambournac, M. Ayre, R. Brenot, H. Benisty, G. Roelkens, T.F. Krauss, D. Van Thourhout, R. Baets, Nanophotonic polarization diversity demultiplexer chip, J. Lightwave Technol. 27 (2009) 417–425.
[3] T. Stomeo, F. Van Laere, M. Ayre, C. Camburnac, H. Benisty, D. Van Thourhout, R. Baets, T.F. Krauss, Integration of grating couplers with a compact photonic crystal demultiplexer on an InP membrane, Opt. Lett. 33 (2008) 884–886.
[4] T. Stomeo, M. Grande, G. Rainò, A. Passaseo, A. D’Orazio, R. Cingolani, A. Locatelli, D. Modotto, C. De Angelis, M. De Vittorio, Optical filter based on two coupled PhC GaAs-membranes, Opt. Lett. 35 (2010) 411–413.
[5] M. Makarova, J. Vuckovic, H. Sanda, Y. Nishi, Silicon-based photonic crystal nanocavity light emitters, Appl. Phys. Lett. 89 (2006) 221101.
[6] G. Shambat, K. Rivoire, J. Lu, F. Hatami, J. Vuckovic, Tunable-wavelength second harmonic generation from GaP photonic crystal cavities coupled to fiber tapers, Opt. Expr. 18 (2010) 12176–12184.
[7] B. Corcoran, C. Monat, C. Grillet, D.J. Moss, B.J. Eggleton, T.P. White, L. O’Faolain, T.F. Krauss, Green light emission in silicon through slow-light enhanced third-harmonic generation in photonic-crystal waveguides, Nat. Photonics 3 (2009) 206–210.
[8] Y.-S. Choi, K. Hennessy, R. Sharma, E. Haberer, Y. Gao, S.P. DenBaars, S. Nakamura, E.L. Hu, C. Meier, GaN blue photonic crystal membrane nanocavities, Appl. Phys. Lett. 87 (2005) 243101.
[9] K. Rivoire, A. Faraon, J. Vuckovic, Gallium phosphide photonic crystal nanocavities in the visible, Appl. Phys. Lett. 93 (2008) 063103.
[10] L. Martiradonna, L. Carbone, A. Tandaechanurat, M. Kitamura, S. Iwamoto, L. Manna, M. De Vittorio, R. Cingolani, Y. Arakawa, Two-dimensional photonic crystal resist membrane nanocavity embedding colloidal dot-in-a-rod nanocrystals, Nanoletters 8 (2008) 260–264.
[11] Y. Gong, J. Vučković, Photonic crystal cavities in silicon dioxide, Appl. Phys. Lett. 96 (2010) 031107.
[12] Si_3N_4 refractive index (n_{SiN}) and extinction coefficient (k_{SiN}) were measured through spectrophotometric and ellipsometric

methods (Woollam M-2000XI ellipsometer) giving value of $n = 1.93$ and $k = 0$ at a wavelength $\lambda = 600$ nm.

[13] V.Em. Vamvakas, N. Vourdas, S. Gardelis, Optical characterization of Si-rich silicon nitride films prepared by low pressure chemical vapor deposition, Microelectron. Reliab. 47 (2007) 794–797.

[14] J. Schmidt, M. Kerr, Highest-quality surface passivation of low-resistivity p-type silicon using stoichiometric PECVD silicon nitride, Sol. Energy Mater. Sol. Cells 65 (2001) 585–591.

[15] D.H. Yoona, S.G. Yoona, Y.T. Kimb, Refractive index and etched structure of silicon nitride waveguides fabricated by PECVD, Thin Solid Films 515 (2007) 5004–5007.

[16] D.S.L. Mui, H. Liaw, A.L. Demirel, S. Strite, H. Morkoç, Electrica characteristics of Si_3N_4/Si/GaAs metal–insulator–semiconductor capacitor, Appl. Phys. Lett. 59 (1991) 2847–2849.

[17] A. Chen, M. Young, W. Li, T.P. Ma, J.M. Woodall, Metal–insulator–semiconductor structure on low-temperature grown GaAs, Appl. Phys. Lett. 89 (2006) 233514.

[18] H. Gaoa, R. Luginbühlb, H. Sigrista, Bioengineering of silicon nitride, Sens. Actuators B Chem. 38 (1997) 38–41.

[19] S. Dauphasa, S. Ababou-Girardb, A. Girardc, F. Le Bihanc, T. Mohammed-Brahimc, V. Viéd, A. Corlue, C. Guguen-Guillouzoe, O. Lavastrea, F. Genestea, Stepwise functionalization of SiN_x surfaces for covalent immobilization of antibodies, Thin Solid Films 517 (2009) 6016–6022.

[20] J. Diao, D. Ren, J.R. Engstrom, K.H. Lee, A surface modification strategy on silicon nitride for developing biosensors, Anal. Biochem. 343 (2005) 322–328.

[21] M. Barth, J. Kouba, J. Stingl, B. Löchel, Oliver Benson, Modification of visible spontaneous emission with silicon nitride photonic crystal nanocavities, Opt. Expr. 15 (2007) 17231–17240.

[22] M. Barth, N. Nüsse, J. Stingl, B. Löchel, Oliver Benson, Emission properties of high-Q silicon nitride photonic crystal heterostructure cavities, Appl. Phys. Lett. 93 (2008) 021112.

[23] M. Eichenfield, R. Camacho, J. Chan, K.J. Vahala, O. Painter, A picogram- and nanometre-scale photonic-crystal optomechanical cavity, Nature 459 (2009) 550–555.

[24] Y. Gong, M. Makarova, S. Yerci, R. Li, M. Stevens, B. Baek, S.W. Nam, L. Dal Negro, J. Vuckovic, Observation of transparency of erbium-doped silicon nitride in photonic crystal nanobeam cavities, Opt. Expr. 158 (2010) 13863–13873.

[25] M. Khan, T. Babinec, M.W. McCutcheon, P. Deotare, M. Lončar, Fabrication and characterization of high-quality-factor silicon nitride nanobeam cavities, Opt. Lett. 36 (2011) 421–423.

[26] L.C. Andreani, G. Panzarini, J.-M. Gérard, Strong-coupling regime for quantum boxes in pillar microcavities: theory, Phys. Rev. B 60 (1999) 13276–13279.

[27] F. Pisanello, G. Leménager, L. Martiradonna, P. Spinicelli, A. Fiore, A. Amo, E. Giacobino, R. Cingolani, M. De Vittorio, A. Bramati, Evaluation of oscillator strength in colloidal CdSe/CdS dots-in-rods, Phys. Status Solidi C 7 (2010) 2688–2691.

[28] E.M. Purcell, Spontaneous emission probabilities at radio frequencies, Phys. Rev. 69 (1946) 681.

[29] F. Pisanello, A. Qualtieri, T. Stomeo, L. Martiradonna, R. Cingolani, A. Bramati, M. De Vittorio, High-Purcell-factor dipolelike modes at visible wavelengths in H1 photonic crystal cavity, Opt. Lett. 35 (2010) 1509–1511.

[30] O. Painter, R.K. Lee, A. Scherer, A. Yariv, J.D. O'Brien, P.D. Dapkus, I. Kim, Two-dimensional photonic band-gap defect mode laser, Science 284 (1999) 1819.

[31] A. Tandaechanurat, S. Iwamoto, M. Nomura, N. Kumagai, Y. Arakawa, Increase of Q-factor in photonic crystal H1-defect nanocavities after closing of photonic bandgap with optimal slab thickness, Opt. Expr. 16 (2008) 448–455.

[32] F. Pisanello, M. De Vittorio, R. Cingolani, Modal selective tuning in a photonic crystal cavity, Superlattices Microstruct. 47 (2010) 34–38.

[33] Match: 5′-Cy3–CTC CCC CAT GCC ATC CTG CG-3′.

[34] Mouse monoclonal Anti-Vinculin, Clone hVIN-1, purchased from Sigma Aldrich.

[35] N. Ganesh, W. Zhang, P.C. Mathias, E. Chow, J.A.N.T. Soares, V. Malyarchuk, A.D. Smith, B.T. Cunningham, Nat. Nanotechnol. 2 (2007) 515–520.

[36] M. Boroditsky, R. Vrijen, T.F. Krauss, R. Coccioli, R. Bhat, E. Yablonovitch, Spontaneous emission extraction and Purcell enhancement from thin-film 2-D photonic crystals, J. Lightwave Technol. 17 (1999) 2096–2112.

[37] S.-H. Kim, S.-K. Kim, Y.-H. Lee, Vertical beaming of wavelength-scale photonic crystal resonators, Phys. Rev. B 73 (2006) 235117–235129.

[38] S.L. Portalupi, M. Galli, C. Reardon, T.F. Krauss, L. O'Faolain, L.C. Andreani, D. Gerace, Planar photonic crystal cavities with far-field optimization for high coupling efficiency and quality factor, Opt. Expr. 18 (2010) 16064–16073.

[39] L. Martiradonna, F. Pisanello, T. Stomeo, A. Qualtieri, G. Vecchio, S. Sabella, R. Cingolani, M. De Vittorio, P.P. Pompa, Spectral tagging by integrated photonic crystal resonators for highly sensitive and parallel detection in biochips, Appl. Phys. Lett. 96 (2010) 113702.

[40] F. Pisanello, L. Martiradonna, P.P. Pompa, T. Stomeo, A. Qualtieri, G. Vecchio, S. Sabella, M. De Vittorio, Parallel and high sensitive photonic crystal cavity assisted read-out for DNA-chips, Microelectron. Eng. 87 (2010) 747–749.

[41] F. Pisanello, L. Martiradonna, P. Spinicelli, A. Fiore, J.P. Hermier, L. Mannab, R. Cingolani, E. Giacobino, M. De Vittorio, A. Bramati, Dots in rods as polarized single photon sources, Superlattices Microstruct. 47 (2010) 165–169.

[42] F. Pisanello, L. Martiradonna, G. Leménager, P. Spinicelli, A. Fiore, L. Manna, J.-P. Hermier, R. Cingolani, E. Giacobino, M. De Vittorio, A. Bramati, Room temperature-dipolelike single photon source with a colloidal dot-in-rod, Appl. Phys. Lett. 96 (2010) 033101.

[43] M. De Vittorio, F. Pisanello, L. Martiradonna, A. Qualtieri, T. Stomeo, A. Bramati, R. Cingolani, Recent advances on single photon sources based on single colloidal nanocrystals, Opto-Electron. Rev. 18 (2010) 1–9.

[44] A. Qualtieri, G. Morello, P. Spinicelli, M.T. Todaro, T. Stomeo, L. Martiradonna, M. De Giorgi, X. Quélin, S. Buil, A. Bramati, J.-P. Hermier, R. Cingolani, M. De Vittorio, Nonclassical emission from single colloidal nanocrystals in a microcavity: a route towards room temperature single photon sources, New J. Phys. 11 (2009) 033025.

[45] Colloidal nanocrystals geometrical parameters: core diameter 2.7 nm, shell length ∼32 nm.

[46] J.M. Rico-Garcia, J.M. Lopez-Alonso, J. Alda, Multivariate analysis of photonic crystal microcavities with fabrication defects, Proc. SPIE 5840 (2005) 562.